Key Engineering Materials
ISSN: 1662-9795, Vol. 926, pp 2342-2354
doi:10.4028/p-g7120f

Submitted: 2021-12-02
Revised: 2022-01-24
Accepted: 2022-01-24
Online: 2022-07-22

Analysis, Prediction and Reduction of Emissions in an Industrial Hot Forming Process Chain for the Manufacture of Sheet Metal Components

M.C. Ghattamaneni[1,a*], S. Wernicke[1,b], T.S. Hainmann[1,c], H. Sulaiman[2,d] and A.E. Tekkaya[1,e]

[1]Institute of Forming Technology and Lightweight Components, TU Dortmund University, Baroper Str. 303, Dortmund 44227, Germany

[2]Faurecia Autositze GmbH, Garbsener Landstraße 7, Hannover 30419, Germany

[a]Manish.Ghattamaneni@iul.tu-dortmund.de, [b]Sebastian.Wernicke@iul.tu-dortmund.de, [c]Till.Hainmann@iul.tu-dortmund.de, [d]Hosen.Sulaiman-dr@faurecia.com, [e]Erman.Tekkaya@iul.tu-dortmund.de,

Keywords: Green Manufacturing, CO_2 Emissions, Sheet Metal Forming, Hot Forming, Heat Recovery.

Abstract. Increasing demands for reducing greenhouse gases drive the metal processing industries to a CO_2-neutral production. A thorough understanding of CO_2 emission sources from the stage of material acquisition up to the final component is thus necessary to improve the CO_2 footprint of sheet metal hot forming process chains. To emphasize on this, an exemplary hot forming process chain is assessed to identify the impact of each sub-process step on total CO_2 emissions and the savings potential of individual measures is evaluated. Moreover, a mathematical model is proposed that enables for the prediction of the product specific CO_2 emissions as early as in the product design stage. This model is tested to calculate the CO_2 emissions resulted during the production of an exemplary hot stamped sheet component. The results point out that the heating stage is responsible for the second highest percentage of CO_2 emissions in the process chain next to the material acquisition. Thus, as one of the most suitable measures, a concept to recover process heat from hot formed components to the cold initial blanks is proposed and evaluated analytically.

Introduction

A driving factor for the climate change are CO_2 emissions, which intensify global warming through the greenhouse gas effect. Political developments, such as the European Union's "Green Deal" reinforce the perception of environmental sustainability in industrial processes. The increasing demand from stakeholders for sustainable investment is seen as a factor pushing companies to implement climate protection measures.

As a part of the industrial sector, companies active in the field of metal processing can contribute to climate protection by analyzing and optimizing their process chains. Dehli (2020) presents a comprehensive tool for increasing industrial energy efficiency [1]. A more specific approach to balance energy and material in sheet metal forming with consideration of efficiency of shearing processes was presented in [2]. The authors considered the CO_2 emissions as initial variables in their analysis.

An overview of sustainability aspects of sheet metal forming with regard to the entire life cycle of a product is described in detail by [3]. The sustainability in the form of a comparison between incremental sheet metal forming and deep drawing in terms of material efficiency and energy use for the manufacture of the same component is presented by [4]. Gao et al. (2019) provides a comprehensive review of energy efficiency in forming processes [5]. The authors initially collected few methods to identify and monitor the necessary energy use of the forming processes. Finally, they presented some concrete approaches to increase the energy efficiency of forming processes using the improvement measures for hydraulic presses. In [6] ways to minimize the CO_2 emissions of a cold forging process based on lubricants and forming operations are considered. They calculated the CO_2 emissions by multiplying the numerically calculated work of the processes by a factor for the

emissions of the power generation. However, the efficiency of the forming presses was not considered.

Modelling of CO_2 emissions based on manufacturing processes is state of the art and models for the calculation of electricity consumption are available in literature. A general approach for calculating the CO_2 emissions of manufacturing processes based on the electricity consumption of the machines in different operating states and the material requirements of the process is shown in [7]. Gao et al. (2017) presents a mathematical model for calculating CO_2 emissions in a sheet metal forming process chain [8]. The authors recorded the individual process steps of material procurement, stamping, transfer, forming and final cutting and then calculated the CO_2 emissions caused in each case from measurements of the energy consumption in a real process chain. The calculation of CO_2 emissions caused during the life cycle of manufacturing tools was presented in [9]. For this purpose, the authors divided the emissions into fixed as well as variable emissions. Accordingly, fixed emissions include CO_2 emissions caused during raw material production, assembly or transport of the tools. Variable emissions include CO_2 emissions caused by the generation of the electricity required to operate the tools. A simulation approach for the influence of disturbances on the dynamic CO_2 emissions of manufacturing processes is described in [10].

This paper provides a special focus on a complete hot forming process chain for sheet metal components. It aims to present options for reducing CO_2 emissions from this process chain that can be applied as universally as possible. Furthermore, this paper investigates to predict the CO_2 footprint of components as simply and accurately as possible in the product-planning phase. Previous models from the literature sources allow the calculations based on the measured energy of the machines used. However, the modular model set up in the context of this paper should make it possible to calculate the CO_2 emissions per component based on the ideal energy required for individual process steps. Based on the results obtained, a concept to recover process heat from hot formed components to the cold initial blanks is proposed. Using a concrete example this concept is computationally tested to verify under which technical conditions it makes sense to recover heat from hot formed components for further use in the process.

Sources of CO_2 Emissions and Saving Potentials in Hot Forming Process Chains

An exemplary hot forming process chain, which contains characteristic steps from the material acquisition to the formed product, along with the emission sources is depicted in Fig. 1. Based on this process chain, four areas are identified for which the potentials for saving CO_2 emissions are evaluated individually. The first area includes all CO_2 emissions during the production of the raw material. All CO_2 emissions generated during the introduction of heat into the process are assigned to a second area. The third area includes all CO_2 emissions caused by the forming operations on presses. All other CO_2 emissions caused by auxiliary systems, such as conveyor belts or robots, decoilers for sheet metal coils or compressed air systems are assigned to the last area. Auxiliary systems can also include lighting, heating, ventilation, and air conditioning of the production facility. On overall, the total emissions can be categorised into three scopes: All CO_2 emissions that are generated during the production of the raw material (indicated as scope 3 emissions), during the generation of the purchased electricity (scope 2 emissions), and directly through combustion processes (scope 1 emissions). Throughout this paper, it is assumed that all machines in the process chain operate continuously at their rated output.

Conventional processes for the production of steel are through blast furnace or electric arc furnace [11]. Hasanbeigi et al. (2016) mentions that for every tonne of steel produced, 1.1 to 2.1 tonnes of CO_2 are released depending on the country of production [12]. These emissions are released during the reduction of iron ores via conventional blast furnace. Production of steel via electric arc furnace is generally more efficient and therefore causes less CO_2 emissions [13]. However, the authors mention that this application is still restricted to the availability of scrap. A drastic reduction in the emissions can be achieved by producing steel using hydrogen direct reduction. However, the steel production via this route is currently under development and is only estimated to be viable with support in the form of subsidies [14]. From the literature sources, it is clear that increasing material

efficiency should therefore have highest priority. Even small improvements in material efficiency, such as avoidance of scrap can result in a comparatively large reduction in CO_2 emissions. For instance, the technology of plate forging, shown in [15], can be used and allows the manufacture of load-optimized components without subsequent machining operations, which saves considerable amount of scrap. Thus, all these aspects have to be examined carefully to achieve the highest possible material efficiency.

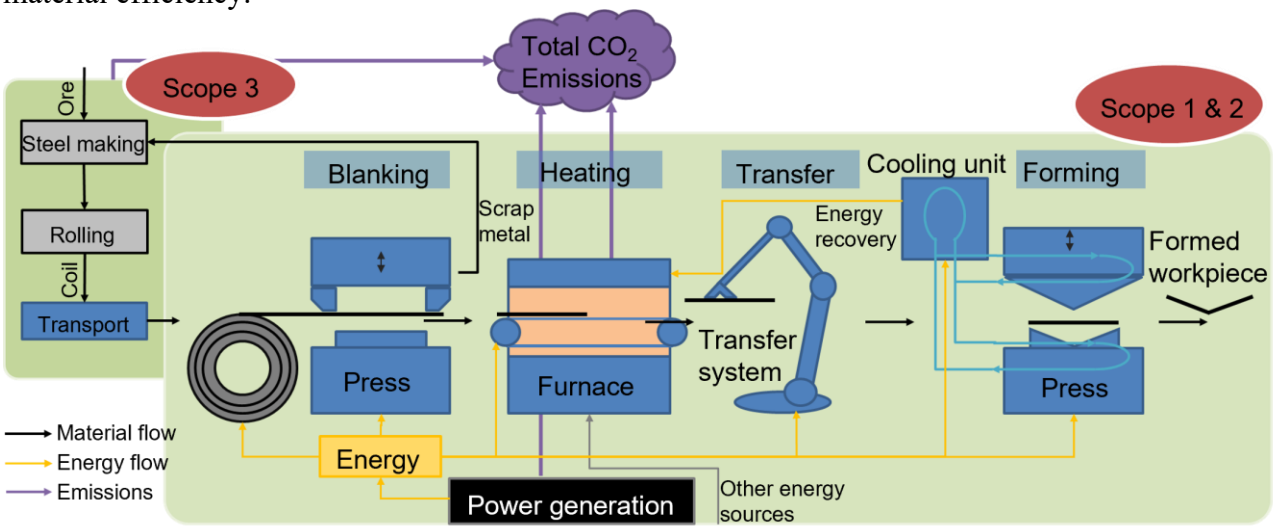

Fig. 1: Exemplary hot forming process chain including CO_2 emission sources

Heating is estimated to be second largest responsible process step for CO_2 emissions. Heat introduced into the process can possibly be recovered. The possibilities of using the recovered heat in the same process should be investigated during production planning phase. An approach for such a possibility is presented in this paper as heat recovery provides the possibility for highest savings in emissions of the process chain (excluding the scope 3 emissions).

The CO_2 emissions of the forming processes are directly proportional to the energy consumed by the forming machines. Thus, the CO_2 emissions depend largely on the energy efficiency of the presses used. For instance, using servo presses has considerable advantage due to their low energy consumption. Kawamoto et al. (2018) compared the energy consumption of servo press with conventional mechanical press for producing different automotive parts [16]. The authors stated that approximately 75% of the reduction in energy consumption can be expected for servo presses when compared to the mechanical presses especially in the standby condition. In the case of hydraulic presses, intermediate storage systems for hydraulic pressure can increase energy efficiency. If several hydraulic presses are used, adapted drive systems for process chains with several presses can reduce the need for electrical energy and thus save CO_2 emissions [17]. If the purchase of new presses is not desired or possible, existing hydraulic or mechanical presses can be possibly converted to servo presses as show in [18].

The total CO_2 emissions of forming tools are summation of the emissions during the manufacturing of the tools and during the usage of the tools. The forming tools are generally machined and thus, the emissions arising from the machining processes have to be taken into account [3]. As implied in [3] it is important to accurately estimate the amount of material necessary for the machining of the tooling, which reduces the CO_2 footprint of the tools. Besides, the forming tools used in hot forming experiences high tool wear, fatigue, and thermal loads compared to that of cold forming ultimately leading to a lower life time of the tools [19]. For instance, using appropriate coatings and by corrective cooling of the tools can lead to an improved tool life. Different state of the art surface modification technologies to improve the performance of hot forming tools is presented by [19]. Studies have also been made to understand the high temperature tribological behaviour of different hot forming tool materials [20]. Thus, choosing the right tool material and improving the process conditions will lead to a lower environmental impact of the hot forming tools during usage.

Auxiliary systems include all other systems that cause CO_2 emissions directly or indirectly through the usage of electrical energy. In transfer systems with electric drives, energy efficiency can be increased by replacing the motors. However, the maximum impact of such measures on the total CO_2 emissions is negligibly low.

Simplified Mathematical Model for the Calculation of the Carbon Footprint of Components

A mathematical model is described in this section that enables the estimation of the CO_2 emissions caused per component as early as in the product development phase. The model is also tested to calculate the component specific CO_2 emissions for an exemplary hot stamped sheet metal component made of 22MnB5 steel, shown in Fig. 2. The component is a typically used gear rack in automobile seats. The details used for the calculations are presented in Table 1.

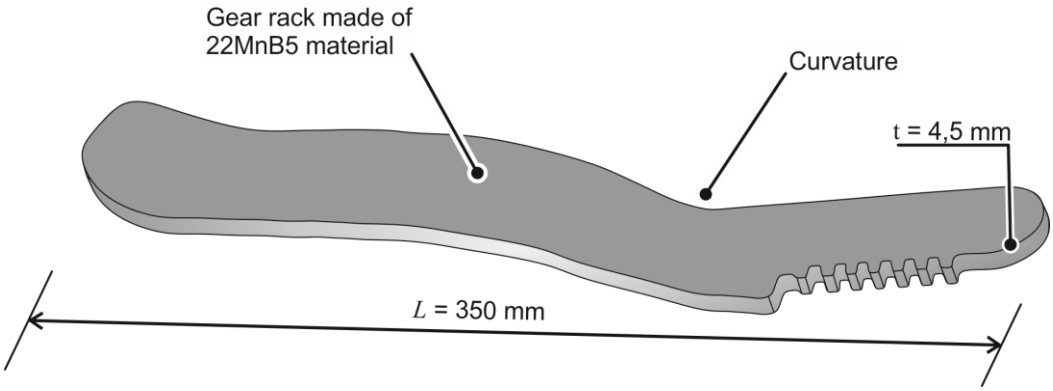

Fig. 2: Pictionary description of an exemplary hot stamped sheet component used for calculations

The basis of this model depends on Eq. 1, which calculates the total CO_2 emissions per component from a process step as the product of the ideal energy W_{id} required for the process step, a factor f_{CO2} for the CO_2 emissions, and the inverse of an efficiency η.

$$Em_{CO_2} = W_{\mathrm{id}} \cdot f_{\mathrm{CO_2}} \cdot \frac{1}{\eta}. \tag{1}$$

The efficiency is a value, which is taken either as an empirical value from measurements of previous, similar processes or from literature sources. The factors for CO_2 emissions are the CO_2 emitted during the production of the electricity required by the machines and the mass-specific CO_2 emissions from material acquisition. In the following, the model describes the total CO_2 footprint of a typical hot stamping process chain (see Fig. 1) from material acquisition to the final formed product in detail for each of the process steps involved.

CO_2 Emissions from Material Acquisition: The CO_2 emissions from raw material production are obtained by multiplying the component mass m_p and the mass of scrap m_{sc} produced per part by the factor for the mass-specific CO_2 emissions from raw material production f_{StPr}, as shown in Eq. 2.

$$Em_{\mathrm{mp}} = \left(m_{\mathrm{p}} + m_{\mathrm{sc}}\right) \cdot f_{\mathrm{StPr}}. \tag{2}$$

CO_2 Emissions from Blanking Process Step: The ideal energy required for blanking processes is obtained by multiplying the average blanking force F_c show in Eq. 3 with the original sheet thickness s_0, which is the cutting path [21]. The required material parameters are the tensile strength R_m and the shear strength factor c_1, which is usually estimated within the values between 0.6 and 0.9 (lower values for brittle, higher for ductile materials) [22].

$$F_{\mathrm{c}} = \frac{2}{3} \cdot s_0 \cdot l_{\mathrm{c}} \cdot c_1 \cdot R_{\mathrm{m}}. \tag{3}$$

According to Eq. 4, the CO_2 emissions of blanking are obtained by multiplying the ideal energy by the factor f_{ElPr} for the CO_2 emissions of power generation and the efficiency η_c, which quantifies the efficiency of the machine used for this process.

$$Em_b = F_c \cdot s_0 \cdot f_{\mathrm{ElPr}} \cdot \frac{1}{\eta_c}. \quad (4)$$

Table 1: Details of the component, material, and process specifications used for the calculations

Component specifications	**Value**
Total mass of the component m_p [kg]	0.5
Mass of the scrap assumed per component m_{sc} [kg]	0.1
Thickness s_0 [mm]	5
Density ρ [g/cm^3]	7.730
Total volume of the component V_p [mm^3]	70000
Material	22MnB5 steel
Material specifications	**Value**
Young's modulus E [GPa]	210
Average yield stress k_{ym} [MPa]	100
Ultimate tensile strength R_m [MPa]	500
Logarithmic strain for the component φ_{pl}	2
Shear strength factor c_1	0.75
Process specifications	**Value**
Process frequency f [components produced/minute]	12
Operating hours t [per year]	3600
Induction heating efficiency η_h	0.5
Blanking efficiency η_c	0.2
Transfer process step efficiency η_m	0.9
Forming efficiency η_f	0.2
Total heating steps n	3
Initial temperature of the blank T_{RT} [° C]	20
Forming temperature T_f [° C]	1100
Number of robots used n_r	4
Number of motors per robot n_m	3
Average motor power P_m [W]	150

CO_2 Emissions from Heating Process Step: The ideal energy for heating of components is given by Eq. 5 [22]. Here, the mass of the components m_p is multiplied by the integral over the specific heat capacity c_p of the material and the process temperatures T_{RT} and T_f as integration limits, which are generally the room temperature and the forming temperature.

$$Q_{id} = m_p \cdot \int_{T_{RT}}^{T_f} c_p(T)dt. \quad (5)$$

Multiplying the ideal energy by the factor for the CO_2 emissions of the heating process (in the case of inductors it is f_{ElPr}) and the efficiency η_h, which quantifies the efficiency of the process used for heating, yields Eq. 6. This is repeated for all n heating steps and the results are summed up.

$$Em_h = m_p \cdot f_h \cdot \sum_{i=1}^{n} \left[\frac{1}{\eta_h^i} \cdot \int_{T_{RT}}^{T_f} c_p(T)dt\right]. \quad (6)$$

CO_2 Emissions from Transfer Process Step: The CO_2 emissions from transfer processes are calculated via the energy consumed by the used robots. The motor power P_m is multiplied by the number of motors per robot n_m and the number of robots n_r. The power determined in this way is integrated over

the operating time per component t. The energy consumption of the robots in standby mode is neglected. The CO_2 emissions from transfer processes are calculated according to Eq. 7 by multiplying the ideal energy of the robots by the factor for the CO_2 emissions of the power generation f_{ElPr} and the efficiency η_{m}, which quantifies the efficiency of the electric motors.

$$Em_{\mathrm{t}} = f_{\mathrm{ElPr}} \cdot \frac{1}{\eta_{\mathrm{m}}} \cdot \int_0^t n_{\mathrm{r}} \cdot n_{\mathrm{m}} \cdot P_{\mathrm{m}}\, dt. \tag{7}$$

CO_2 Emissions from Forming Process Step: The ideal energy of forming processes is given by Eq. 8, where V_{p} is the volume of the component to be formed, k_{y} is its yield stress, and φ_{pl} is the logarithmic strain.

$$W_{\mathrm{id}} = \int_{V_{\mathrm{p}}} \int_0^{\emptyset_{\mathrm{pl}}} k_{\mathrm{y}} \cdot d\varphi_{\mathrm{pl}} \cdot dV_{\mathrm{p}}. \tag{8}$$

The CO_2 emissions of the forming process are calculated according to Eq. 9 by multiplying the ideal energy W_{id} with the factor f_{ElPr} for the CO_2 emissions and the efficiency η_{f}, which quantifies the efficiency of the machine used for forming. As the yield stress is a non-linear function of the effective plastic strain but hot forming stops strain hardening, a simplified mean k_{ym} is used.

$$Em_{\mathrm{f}} = V_{\mathrm{p}} \cdot k_{\mathrm{ym}} \cdot \varphi_{\mathrm{pl}} \cdot f_{\mathrm{ElPr}} \cdot \frac{1}{\eta_{\mathrm{f}}}. \tag{9}$$

CO_2 Footprint of the Tools: The individual calculation of the CO_2 footprint for tools is not provided within the framework of this model. The influence on the component-specific CO_2 emissions is calculated according to Eq. 10 by dividing the CO_2 footprint of the tool cf_{die} with the total number of parts that can be produced with the tool n_{p}.

$$Em_{\mathrm{die}} = \frac{cf_{\mathrm{die}}}{n_{\mathrm{p}}}. \tag{10}$$

The parameter n_{p} is taken here as 2.6 million parts, which is estimated based on the experience. This parameter is decided considering the whole hot forming tool system. Nevertheless, the active forming surfaces, i.e. the tool inserts will be worn considerably faster and is replaced frequently compared to the whole tool system. Ultimately, the lifespan of the forming tools is largely depending upon the forming processes and their conditions and thus n_p is to be estimated accordingly.

Summation of all the above equations will result in the total carbon footprint of the process chain as shown in Eq. 11.

$$Em_{\mathrm{total}} = Em_{\mathrm{mp}} + Em_{\mathrm{b}} + Em_h + Em_{\mathrm{t}} + Em_{\mathrm{f}} + Em_{\mathrm{die}}. \tag{11}$$

Results. With an implementation of above mentioned model and the described specifications (see Table 1) in MATLAB a fast variation of parameters and comparison of results is possible. The results of the total CO_2 emissions obtained for the component (see Fig. 2) are shown in the form of a pie chart in Fig. 3a. In addition, Fig. 3b shows the component specific CO_2 emissions excluding the emissions caused by the raw material production.

The component specific CO_2 emissions Em_{total} for this sheet metal component amount to a total of 1189 g. The highest proportion of CO_2 emissions is caused by raw material production, which amounts 88.27% and thus leads to a total of 1049 g. All the direct CO_2 emissions released and the emissions released because of consumed electricity of the process chain add up to 140 g (see Fig. 3b).

It is assumed that the raw material used in the model does not contain any recycled content in it. Besides, the model only accounts for the scrap produced per component ignoring the step of scrap recycling. However, in reality the scrap is in turn recycled and this will lead to decrease in the total

emissions considerably depending upon the efficiency of recycling. Thus, it should be aimed to achieve the highest scrap recycling efficiency as this would significantly improve the environmental impact of the process chain. Ultimately, the simplified model presents an upper bound regarding the resulting CO_2 emissions.

Next to the material production stage, it can be clearly seen that the heating operation is responsible for a large proportion of the CO_2 emissions caused (91.03%). The forming process itself only causes approx. 6% of CO_2 per component. The process steps of blanking, transfer and tool manufacturing combined cause only around 3% of CO_2 per component. It should be noted that overall experience and product dependent assumptions have been made for calculating the tool emissions, however the proportion of the tool emissions is overall negligible (see Fig. 3b). Ultimately, the results point out that next to the material saving the heat recovery should be the priority for reducing the carbon footprint of these process chains. Therefore, a heat recovery concept that is plausible within this process chain is proposed, evaluated analytically, and is discussed in the following chapter.

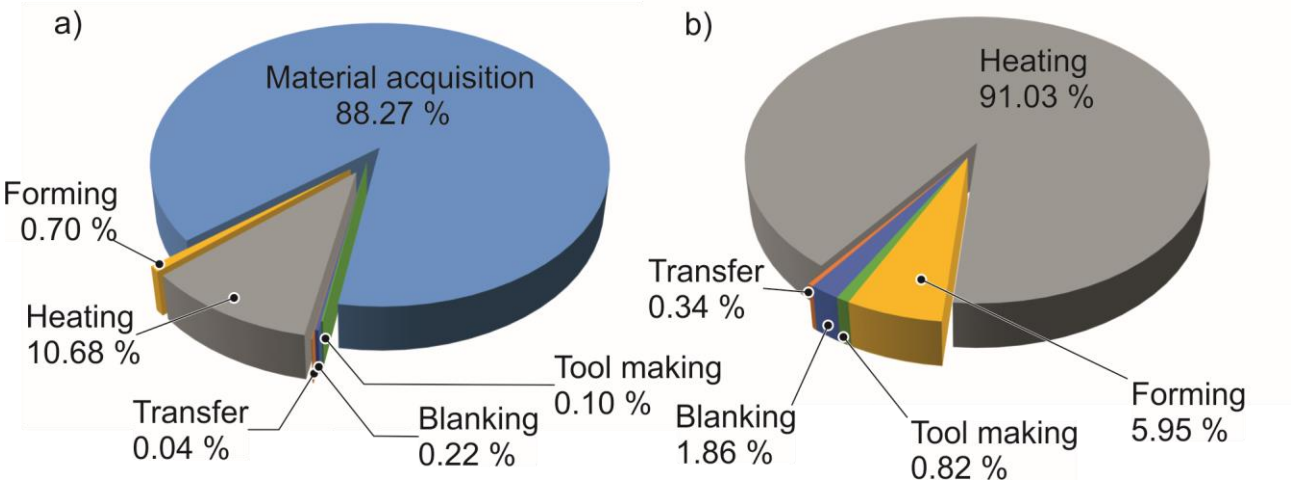

Fig. 3: a) Shares of the total CO_2 emissions for the exemplary component, b) Shares of the CO_2 emissions excluding the material acquisition stage

A critical aspect of the results shown is that the estimation of the efficiencies, in particular of the blanking and forming processes, can result in large inaccuracies. In the calculation of the above-mentioned results, these efficiencies were estimated at 20%. However, considerably lower efficiencies are conceivable, especially for small blanking and forming forces, if presses with high maximum capacity are used. It is therefore advisable to determine the machine equipment specific empirical values for the efficiencies.

Investigation on Heat Recovery for Preheating Cold Blanks

A typical industrial hot stamping process is schematically shown in Fig. 4. In the first step, blanks of suitable sizes are obtained from a sheet metal coil (provided by the supplier) from the blanking operation. Then, an inductive unit preheats each blank from room temperature (RT) to a temperature of 150 °C in order to apply a scaling protecting agent (coating). Later, the heating unit heats it up until 1100 °C. After forming, the temperature of the blank amounts approx. 800 °C and rapidly drops in a quench tank to 200 °C to reach a martensitic microstructure. A subsequent annealing process is performed to temper the martensitic structure formed in the component. Thus, the heating unit heats the formed component again to 400 °C and this component is then cooled in air.

In the whole process, quenching leads to the highest heat loss. Heat recovery of the steam at this point is difficult because of the continuous and open system. Thus, this paper focuses the heat that can be recovered from the final annealing process. The aim is transfer the heat from the formed components to the initial cold blanks in order to avoid the first step of the process, i.e. inductive preheating of the blanks from RT to 150 °C.

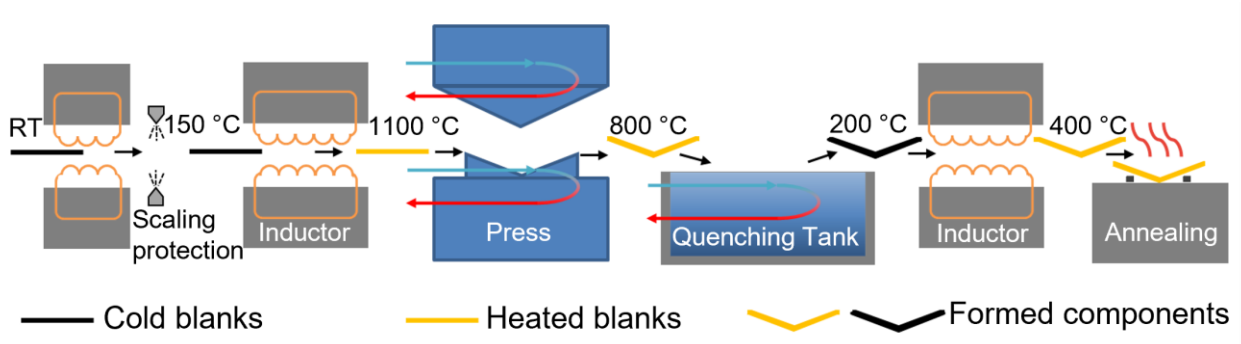

Fig. 4: Typical industrial hot stamping process with temperature of the blank/ component at each stage

The heat transfer medium considered for this concept is dry air and the mechanism of heat transfer is forced convection. The paper also analyses two configurations: parallel flow and counter flow configurations as shown in Fig. 5a and Fig. 5b respectively. The heat recovery consists of two steps, first the heat transfers from the hot components to the air stream (channel 1). In a second step, the heated air stream transfers this heat to the following cold blanks (channel 2). It is assumed that the hot components and the cold blanks are each moved through channels (0.05 m² in cross-sectional area) 1 and 2 respectively using conveyor belts. The velocity of these belts are determined depending upon the process frequency *f*. Besides, it is assumed that there is no heat transfer to the conveyor belts. The heat flux for convective heat transfer is calculated according using Eq. 12 as shown in [23].

$$\dot{Q} = \alpha \cdot A \cdot \left(T_{1,\mathrm{x}} - T_{2,\mathrm{x}}\right). \tag{12}$$

The heat transfer coefficient α takes into consideration the material parameters of the heat transfer medium and process parameters. A is the surface area used for heat transfer. The notations for the temperatures in this paper are represented in the form of $T_{\mathrm{i,x}}$, where the subscript i represents the material and the subscript x represents the channel. The subscript i is replaced with 1 for hot material and 2 for cold material respectively. For instance, $T_{1,1}$ is the temperature of the hot component and $T_{2,1}$ is the temperature of the cold air in channel 1. Whereas, $T_{1,2}$ is the temperature of hot air and $T_{2,2}$ the temperature for cold blanks in channel 2.

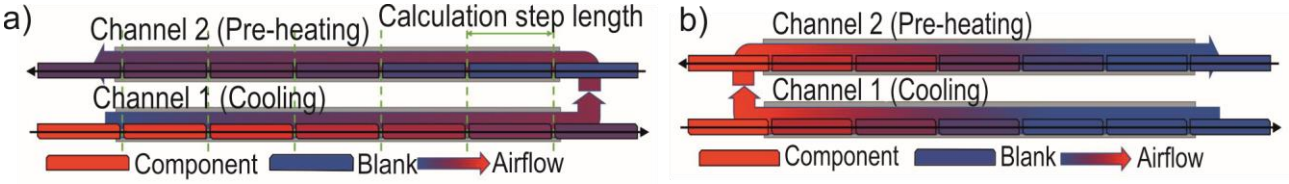

Fig. 5: Heat recovery concept using a) parallel flow configuration, b) counter flow configuration

The heat transfer coefficient α can be determined by converting Eq. 13 via the dimensionless Nusselt number *Nu*. This number is determined as a function of the fluidic flow concept from empirically or semi-empirically determined correlations. In this paper, two concepts are analysed depending upon the airflow: first "turbulent flow along a flat plate" and second "turbulent thermally and hydro dynamically formed flow through pipes" (also known as "channel flow"). In addition, the length l of the fluid flow and the thermal conductivity λ of the fluid must be known.

$$Nu = \frac{\alpha \cdot l}{\lambda}. \tag{13}$$

If the airflow concept is considered to be a turbulent flow along a flat plate ($5\times10^5 < Re < 10^7$), the Nusselt number is calculated according to Eq. 14. The Prandtl number *Pr* depends on the heat transfer medium used and can be taken from tables in [23].

$$Nu = \frac{0.037 \cdot Re^{0.8} \cdot Pr}{1+2.443 \cdot Re^{-0.1}\left(Pr^{2/3}-1\right)}. \quad (14)$$

If the airflow concept is considered to be a turbulent thermally and hydro dynamically developed flow through pipes ($10^4 < \mathrm{Re} < 10^6$), the Nusselt number is calculated according to Eq. 15, where L is used as the channel length and d as the hydraulic diameter of the channel.

$$Nu = \frac{Re \cdot Pr \cdot \zeta/8}{1+12.7 \cdot \sqrt{\zeta/8} \cdot \left(Pr^{2/3}-1\right)} \cdot \left[1 + \left(\frac{d}{L}\right)^{2/3}\right]. \quad (15)$$

The coefficient ζ is given by Eq. 16 as per [23].

$$\zeta = (1.8 \cdot \log_{10} Re - 1.5)^{-2}. \quad (16)$$

The Reynolds number Re is a dimensionless number in fluid mechanics, which is calculated according to Eq. 17. The kinematic viscosity v is required, which can be determined from tables such as in [23].

$$Re = \frac{w \cdot l}{v}. \quad (17)$$

Calculation Methods and Results. The final temperature to which the cold blanks can be heated from the recovered heat is a function of the airflow velocity w and the length of the channels L used. Thus, these two parameters are used as variables in the calculations. The details used for the calculations are shown in Table 2. Besides, this paper also analyses two calculation methods for the heat recovery concept. One is step-by-step calculation method and the other is number of transfer units (NTU) method.

Table 2: Details pertaining to the calculations made for the heat recovery concept

Air specifications	**Value**
Airflow initial temperature [°C]	22
Component and Blank specifications	**Value**
Component initial temperature [°C]	400
Component mass m [kg]	0.5
Component length l [mm]	300
Component surface area A [mm^2]	14000
Blank initial temperature [°C]	22
Channel specifications	**Value**
Channel height h [mm]	50
Channel width b [mm]	100

Step-by-step Calculation Method. In this method, the channels are conceptually divided into several sections; each section equal to length of the component (see Fig. 5a) and the moving components are assumed as mass flow $\dot{m}$. As can be observed from Fig. 5a for parallel flow configuration, it is assumed that the air passes over in the same direction as of the components. Firstly, for the first section in the channel 1, the heat flux from the hot components to the airflow is calculated according to Eq. 12 depending upon the airflow concept. Then, using Eq. 18, the new temperature T_{after} of the component and the air because of the heat transfer is calculated. The specific heat capacity c_{p} can be determined experimentally for materials or can be taken from the property tables in [23].

$$\dot{Q} = \dot{m} \cdot c_{\mathrm{p}} \cdot (T_{\mathrm{after}} - T_{\mathrm{before}}). \quad (18)$$

The similar procedure is performed for every section until the end of channel 1. Ultimately, this iterative procedure gives the final temperatures of the hot component and air by the end of channel 1. Subsequently, the same calculation is performed for channel 2 until the complete length of channel 2 is reached. This yields in the final temperatures of the blank and air. Fig. 6a shows the final temperatures of the hot component and air along the length of channel 1. Fig. 6b shows the final temperatures of the blank and air along the length of channel 2.

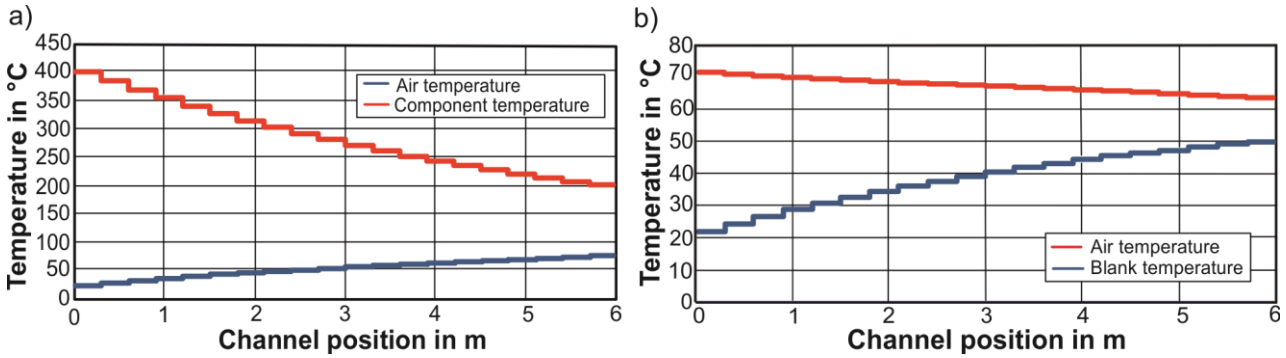

Fig. 6: Temperature development of a) hot component and air along channel 1, b) air and blank along channel 2

The figures indicate that for fixed channel lengths of 6 m, the final temperature of the blank is around 50 °C (see Fig. 6b). This is insufficient for the coating of the blank which requires a temperature of 150 °C. Thus, the parallel flow configuration is not found to be a satisfying configuration corresponding to the result required. Therefore, counter flow configuration is analysed. As the step-by-step calculation method is a forward iterative procedure, it cannot be used for the counter flow configuration as it would lead to mathematical inconsistent solution. Thus, the NTU calculation method is used for this purpose.

NTU Calculation Method. NTU calculation method is a procedure generally used for designing or re-calculating heat exchangers [23]. In this work, the NTU method is also used for the parallel flow configuration in order to compare the results obtained from the step-by-step calculation method.

The calculations and equations used for this method are applied as shown in [23]. First, the heat transfer coefficient α is calculated from Eq. 13. The dimensionless temperature change $\theta_{\mathrm{i,x}}$ is used for calculating the outlet temperatures of the required material in the respected channel. $TE_{1,\mathrm{x}}$ represents the inlet temperature of the hot material at the start of the channel x and $TO_{1,\mathrm{x}}$ represents the outlet temperature of the hot material at the end of the channel x respectively. Ultimately, the outlet temperature of the hot material $TO_{1,\mathrm{x}}$ is obtained by converting the dimensionless temperature change $\theta_{1,\mathrm{x}}$ according to Eq. 19.

$$\theta_{1,\mathrm{x}} = \frac{TE_{1,\mathrm{x}} - TO_{1,\mathrm{x}}}{TE_{1,\mathrm{x}} - TE_{2,\mathrm{x}}}. \tag{19}$$

The outlet temperature of the cold material $TO_{2,\mathrm{x}}$ is obtained by converting the dimensionless temperature change $\theta_{2,\mathrm{x}}$ according to Eq. 20.

$$\theta_{2,\mathrm{x}} = \frac{TO_{2,\mathrm{x}} - TE_{2,\mathrm{x}}}{TE_{1,\mathrm{x}} - TE_{2,\mathrm{x}}}. \tag{20}$$

The values $\theta_{\mathrm{i,x}}$ can be calculated according to Eq. 21 for parallel flow.

$$\theta_{\mathrm{i,x}} = \frac{1 - e^{[-(1+R_i)\cdot NTU_i]}}{1+R_i}. \tag{21}$$

Similarly, the values $\theta_{i,x}$ are obtained for the counter flow configuration as shown in Eq. 22.

$$\theta_{i,x} = \frac{1-e^{[(R_i-1)\cdot NTU_i]}}{1-R_i\cdot e^{[(R_i-1)\cdot NTU_i]}}. \quad (22)$$

In equations Eq. 21 and Eq. 22, the dimensionless coefficient NTU_i and the respective heat capacity current ratio R_i are required. Thus, the dimensionless coefficient NTU_i is calculated using Eq. 23, where $\dot{m}_i$ is the mass flow and c_{pi} is the heat capacity of the respective material.

$$NTU_i = \frac{\alpha\cdot A}{\dot{m}_i\cdot c_{pi}}. \quad (23)$$

The heat capacity current ratio R_1 is obtained from Eq. 24.

$$R_1 = \frac{\dot{m}_1\cdot c_{p1}}{\dot{m}_2\cdot c_{p2}}. \quad (24)$$

The reciprocal of R_1 is used for the heat capacity current ratio R_2 (see Eq. 25).

$$R_2 = \frac{1}{R_1}. \quad (25)$$

The final temperatures of the blanks as calculated from the NTU method for parallel flow configuration and the counter flow configuration are shown in Fig. 7a and Fig. 7b respectively.

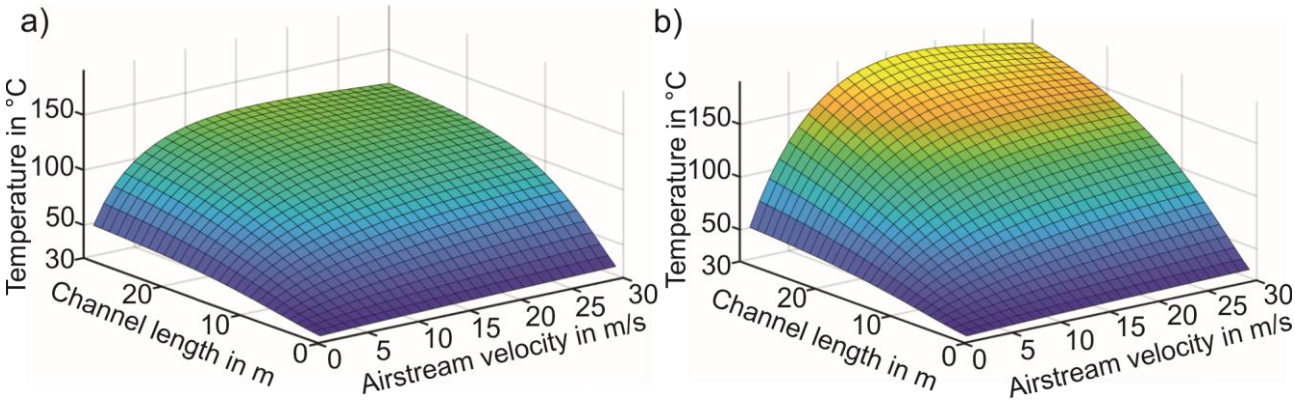

Fig. 7: Temperature of the initial blanks at the end of the channel 2 a) in parallel flow, b) in counter flow configuration

It is observed that the results from the NTU method for the parallel flow configuration only differ by a maximum of 5% from the step-by-step method. It can also be observed that significantly higher output temperatures and also the required 150 °C can be achieved when the counter flow configuration is used (see Fig. 7b). However, the required temperatures are only reached with channel lengths of at least 21 m, which would mean a high demand for production space. Another critical aspects are that dissipation and losses of the air stream mass in the channels are not taken into account. Furthermore, the calculation using this method does not produce a temperature curve over the entire channel length as in the, step-by-step calculation method, but directly the respective output temperatures of the materials at the end of the channels.

Conclusion and Outlook

CO_2 emissions are caused along the process chain during material acquisition, indirectly during the generation of purchased electrical energy or directly during the combustion of fossil fuels. Summarized approaches and technologies to reduce the CO_2 emissions caused were presented and classified in this paper. A mathematical model is presented which enables the calculation of component specific CO_2 emissions as early as the product-planning phase based on the ideal energy required. Based on the model it can be concluded that:

- Raw material production is responsible for the largest part of the CO_2 emissions in the process chain and increasing material efficiency offers the most promising saving potential.
- Influences of individual process parameters on the component specific CO_2 emissions can be analyzed and can even be considered before production. This enables to improve the emissions along the process chain or to check the impact of improvement measures on the total CO_2 emissions.

Furthermore, within the framework of the thermodynamic analysis of an example process, it is possible to develop an analytical model to determine the technical conditions under which the preheating of cold blanks with the aid of recovered heat can be implemented. The computational results of this paper are based on a fictional process chain that was aimed to be as universal as possible. Future investigations aim to verify the results by a real process chain. In addition, the possibilities of heat recovery will be examined mathematically in all other process steps that can be assigned to process heat.

References

[1] M. Dehli, Energieeffizienz in Industrie, Dienstleistung und Gewerbe, Springer, Wiesbaden, 2020.

[2] A. Göschel, A. Sterzing, J. Schönherr, Balancing procedure for energy and material flows in sheet metal forming, CIRP Journal of Manufacturing Science and Technology 4 (2011) 170-179.

[3] G. Ingarao, R. Di Lorenzo, F. Micari, Sustainability issues in sheet metal forming processes: an overview, Journal of Cleaner Production 19 (2011) 337-347.

[4] G. Ingarao, G. Ambrogio, F. Gagliardi, R. Di Lorenzo, A sustainability point of view on sheet metal forming operations: material wasting and energy consumption in incremental forming and stamping processes, Journal of Cleaner Production 29-30 (2012) 255-268.

[5] M. Gao, K. He, L. Li, Q. Wang, C. Liu, A Review on Energy Consumption, Energy Efficiency and Energy Saving of Metal Forming Processes from Different Hierarchies, Processes 7 (2019) 357.

[6] P. Nava, Minimizing Carbon Emissions in Metal Forming, Master thesis, Queen's University, Ontario, 2009.

[7] Y. Wang, H. Zhang, Z. Zhang, J. Wang, Development of an Evaluating Method for Carbon Emissions of Manufacturing Process Plans, Discrete Dynamics in Nature and Society (2015).

[8] M. Gao, H. Huang, X. Li, Z. Liu, Carbon emission analysis and reduction for stamping process chain, International Journal of Adv. Manuf. Tech. 91 (2017) 667-678.

[9] H. Cao, H. Li, H. Cheng, Y. Luo, R. Yin, Y. Chen, A carbon efficiency approach for life-cycle carbon emission characteristics of machine tools, Journal of Cleaner Production 37 (2012) 19-28.

[10] H. Cao, H. Li, Simulation-based approach to modeling the carbon emissions dynamic characteristics of manufacturing system considering disturbances, Journal of Cleaner Production 64 (2014) 572-580.

[11] K. R. Hegemann, R. Guder, Stahlerzeugung., Springer, Wiesbaden, 2020.

[12] A. Hasanbeigi, M. Arens, J. CR. Cardenas, L. Price, R. Triolo, Comparison of carbon dioxide emissions intensity of steel production in China, Germany, Mexico, and the United States, Resources, Conservation and Recycling 113 (2016) 127-139.

[13] T. Fleiter, B. Schlomann, W. Eichhammer, Energieverbrauch und CO_2- Emissionen industrieller Prozesstechnologien, Einsparpotenziale, Hemmnisse und Instrumente, Fraunhofer-Verl., Stuttgart, 2013.

[14] M. Weigel, M. Fischedick, J. Marzinkowski, P. Winzer, Multicriteria analysis of primary steelmaking technologies, Journal of Cleaner Production 112 (2016) 1064-1076.

[15] M. Merklein, H. Hagenah, T. Schneider, Sheet-Bulk Metal Forming Processes – State of the Art and its Perspectives, in: R. Kolleck (Eds.), TTP 2013 – Tools and Technologies for Processing Ultra High Strength Materials, Verlag der TU Graz, 2013.

[16] K. Kawamoto, H. Ando, K. Yamamichi, Application of servo presses to metal forming processes, Procedia Manufacturing 15 (2018) 31-38.

[17] X. Yan, B. Chen, Energy-Efficiency Improvement and Processing Performance Optimization of Forging Hydraulic Presses Based on an Energy-Saving Buffer System, Applied Sciences 10 (2020) 6020.

[18] Y. S. Sun, J. G. Hu, H. B. Zheng, J. P. He, Y. Fang, W. P. Ruan, Energy Saving Drive for Forming Equipments, AMR 154-155 (2010) 701-707.

[19] R. Muvunzi, D. Dimitrov, S. Matope, L. Mugwagwa, Application of surface modification technologies to improve performance of hot sheet metal forming tools: A review, ACRID (2017) 65-74.

[20] S. Hernandez, J. Hardell, H. Winkelmann, M. Rodriguez Ripoll, B. Prakash, Influence of temperature on abrasive wear of boron steel and hot forming tool steels, Wear 338-339 (2015) 27-35.

[21] P. Demmel, R. Golle, H. Hoffmann, R. Petry, Schneiden, in: K. Siegert (Ed.), Blechumformung, Springer, Berlin, 2015.

[22] E. Doege, B. A. Behrens, Handbuch Umformtechnik, Springer, Berlin, 2016.

[23] B. Spring, W. Roetzel, Berechnung von Wärmeüberträgern, in: VDI-Gesellschaft (Ed.), VDI-Wärmeatlas, Springer, Berlin, 2013.